WRDC-TR-89-2079

ELECTRON BEAM GENERATION BY ELECTRON BOMBARDMENT INDUCED CATHODE EMISSION

J.J. Rocca, B. Szapiro, C. Murray

Electrical Engineering Department
Colorado State University
Fort Collins, CO 80523

July 7, 1989

Final Report for Period April '88 - July '89

AERO PROPULSION AND POWER LABORATORY
WRIGHT RESEARCH DEVELOPMENT CENTER
AIR FORCE SYSTEMS COMMAND
WRIGHT-PATTERSON AIR FORCE BASE, OHIO 45433-6563

NOTICE

When Government drawings, specifications, or other data are used for any purpose other than in connection with a definitely Government-related procurement, the United States Government incurs no responsibility or any obligation whatsoever. The fact that the government may have formulated or in any way supplied the said drawings, specifications, or other data, is not to be regarded by implication, or otherwise in any manner construed, as licensing the holder, or any other person or corporation; or as conveying any rights or permission to manufacture, use, or sell any patented invention that may in any way be related thereto.

This report is releasable to the National Technical Information Service (NTIS). At NTIS, it will be available to the general public, including foreign nations.

This technical report has been reviewed and is approved for publication.

ALAN GARSCADDEN
Power Components Branch
Aerospace Power Division
Aero Propulsion Laboratory

L. D. MASSIE, Chief
Power Components Branch
Aerospace Power Division
Aero Propulsion Laboratory

FOR THE COMMANDER

W. U. BORGER, Chief
Aerospace Power Division
Aero Propulsion Laboratory

If your address has changed, if you wish to be removed from our mailing list, or if the addressee is no longer employed by your organization please notify WRDC/POOC, WPAFB, OH 45433-6563 to help us maintain a current mailing list.

Copies of this report should not be returned unless return is required by security considerations, contractual obligations, or notice on a specific document.

UNCLASSIFIED

SECURITY CLASSIFICATION OF THIS PAGE

REPORT DOCUMENTATION PAGE

Form Approved OMB No. 0704-0188

1a. REPORT SECURITY CLASSIFICATION: UNCLASSIFIED	1b. RESTRICTIVE MARKINGS: N/A
2a. SECURITY CLASSIFICATION AUTHORITY: N/A	3. DISTRIBUTION/AVAILABILITY OF REPORT: Approved for Public Release: Distribution Unlimited
2b. DECLASSIFICATION/DOWNGRADING SCHEDULE: N/A	
4. PERFORMING ORGANIZATION REPORT NUMBER(S): N/A	5. MONITORING ORGANIZATION REPORT NUMBER(S): WRDC-TR-89-2079
6a. NAME OF PERFORMING ORGANIZATION: Colorado State University; 6b. OFFICE SYMBOL (If applicable):	7a. NAME OF MONITORING ORGANIZATION: (WRDC/POOC) Aero Propulsion and Power Laboratory Wright Research and Development Center
6c. ADDRESS (City, State, and ZIP Code): Fort Collins Colorado 80523	7b. ADDRESS (City, State, and ZIP Code): Wright-Patterson AFB Dayton, Ohio 45433-6563
8a. NAME OF FUNDING/SPONSORING ORGANIZATION: SDIO; 8b. OFFICE SYMBOL (If applicable):	9. PROCUREMENT INSTRUMENT IDENTIFICATION NUMBER: F33615-86-C-2723
8c. ADDRESS (City, State, and ZIP Code): Pentagon Washington, D.C. 20301-7100	10. SOURCE OF FUNDING NUMBERS: PROGRAM ELEMENT NO. 1D; PROJECT NO. 1D01; TASK NO 0001; WORK UNIT ACCESSION NO.

11. TITLE (Include Security Classification)

Electron Beam Generation by Electron Bombardment Induced Cathode Emission

12. PERSONAL AUTHOR(S)

J.J. Rocca, B. Szapiro, and C. Murray

13a. TYPE OF REPORT	13b. TIME COVERED	14. DATE OF REPORT (Year, Month, Day)	15. PAGE COUNT
Final	FROM 4/88 TO 2/89	7 July 1989	38

16. SUPPLEMENTARY NOTATION

17. COSATI CODES			18. SUBJECT TERMS (Continue on reverse if necessary and identify by block number)
FIELD	GROUP	SUB-GROUP	
20	09		Cathodes, Silver-Magnesium, Microseconds, Oscillations
09	03		

19. ABSTRACT (Continue on reverse if necessary and identify by block number)

It has been demonstrated that pulsed electron beams can be created by multiplication of a lower current density primary beam impinging on high electron yield targets, similar to those used in photomultiplier tubes. The main results obtained are the generation of : a 17 ampere, 1 microsecond duration beam from a 2.5 cm diameter silver-magnesium polycrystalline alloy target by multiplication of a 2.5 ampere primary beam; implementation of a surface activation technique for Ag-Mg targets that allows reproducible yields up 5.

20. DISTRIBUTION/AVAILABILITY OF ABSTRACT: ☒ UNCLASSIFIED/UNLIMITED ☐ SAME AS RPT. ☐ DTIC USERS	21. ABSTRACT SECURITY CLASSIFICATION: UNCLASSIFIED
22a. NAME OF RESPONSIBLE INDIVIDUAL: Alan Garscadden	22b. TELEPHONE (Include Area Code): 513-255-2923; 22c. OFFICE SYMBOL: WRDC/POOC-3

DD Form 1473, JUN 86 *Previous editions are obsolete.*

SECURITY CLASSIFICATION OF THIS PAGE

UNCLASSIFIED

PROJECT SUMMARY

We have demonstrated that pulsed electron beams can be created by multiplication of a lower current density primary beam impinging on high electron yield targets of the same type previously used to multiply microamp electron currents in photomultiplier tubes. The main results obtained during this Project are the following:

- Generation of a 17-A, 1-μs beam from a 2.5-cm-diameter Ag (98.3%) - Mg (1.7%) polycrystalline alloy target by electron multiplication of a 2.5-A primary beam.

- Implementation of a surface activation technique for Ag-Mg targets that allows to attain reproducible yields greater than 5, which remain stable under bombardment with high primary beam current densities ($\approx$ A/cm^2). Yields up to 7 were occasionally observed.

- Observation of the onset of electron current oscillations, probably associated with the development of beam-plasma instabilities at the relatively low ($<$ 15 keV) acceleration energies used in this work to propagate the electron streams. The maximum electron beam currents obtained were only limited by the appearance of the oscillations, which might be due to electron-ion instabilities associated with the propagation

of high current density quasi-neutralized electron streams. Increasing the acceleration voltage should allow for the generation significantly larger stable currents by electron multiplication.

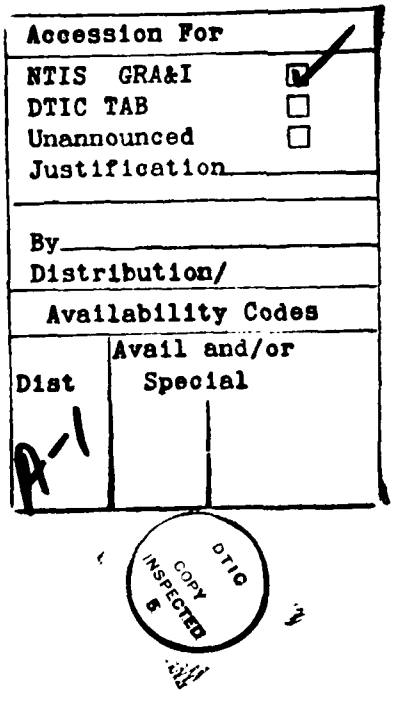

I. INTRODUCTION

We have demonstrated a new approach for the generation of broad area intense electron beams based on the multiplication of electron streams achieved by bombarding high yield materials [1]. This well known phenomenon has been employed for decades in photomultiplier detectors to amplify currents in the submilliamp range [2], but to our knowledge has never been used for the generation of intense electron beams. We generated a broad area electron beam pulses of 1 μsec duration with current densities up to 3.4 A/cm^2 by single stage multiplication of a 0.5-A/cm^2 electron stream. The scheme has the potential of generating intense electron beams whose current and pulse-width are tailored by controlling a low current density beam.

Ion and photon fluxes have been previously used to cause intense electron emission from cold cathodes. The emission of electrons from cathode materials following the bombardment by energetic ions has been widely used in the generation of broad area electron beams [3-8]. While many cathode materials exist which present high electron yields following the bombardment by ions [9,10], ion bombardment electron guns have limitations for the generation of very high current density beams. For a given electron yield, the electron beam current density is limited by the bombarding ion flux, which is itself limited by the large positive space charge. Also, ion bombardment induced sputtering of the cathode material is an undesirable effect that is present and

limits the electron gun lifetime.

Recently, very large electron beam current densities have been achieved using photocathodes [11,12]. The photoemission scheme has the advantages that photons do not present space charge limitations nor cause sputtering. An additional advantage of photocathodes is the very small energy spread of the emitted beam produced by monochromatic irradiation. However, the laser required as a photon source increases the size and complexity of the cathode, and also limits its scaling to very broad areas.

The electron beam was generated by electron bombardment induced emission of an activated Ag-Mg target 2.5 cm in diameter. In this scheme, the electrons emitted by a low current density primary electron source impinge on a high electron yield target at an energy close to that required for maximum emission of secondary electrons. The secondary electrons are subsequently accelerated in the opposite direction to form a higher current density beam. Electrons cause negligible sputtering and create a space charge which is two orders of magnitude lower than that corresponding to an ion beam of the same flux and energy. Some of the same materials and surface activation procedures developed for electron multiplication of the microamp level in photomultiplier tubes allow for efficient electron multiplication at pulsed current densities many orders of magnitude larger. Consequently, the scheme has the potential of generating very high current density pulsed electron beams.

II. EXPERIMENTAL SETUP

II.1. Primary electron gun and target systems

The experimental setup used is schematically shown in Figure 1. The primary, or seed, electron beam pulse is generated from a 2.5-cm-diameter, 2.5 cm-long, thermionic dispenser cathode [13] by pulsing an accelerating grid to positive potential with respect to the cathode. Subsequent acceleration of the beam is achieved floating the setup negatively with respect to a grounded grid. A floating molybdenum cylinder surrounds the dispenser cathode to reduce side emission and radiative heat losses, shielding effectively the cathode from the vacuum chamber and helping reduce dispenser cathode poisoning effects associated with the ionization of background contaminants from the chamber's wall by the electron beam. Figure 2(a) is a photograph of the entire system, including the pulser circuit and vacuum chamber. The photograph in Figure 2(b) shows the thermionic cathode in operation and the target.

The beam generated by the thermionic gun propagates to another grounded grid placed in close proximity with the target. The 70 percent transmissivity grids are made by etching of a 0.010 inch molybdenum sheet [14], allowing for a very good thermal conductivity and mechanical stability. The target is negatively biased with respect to ground to retard the electrons from the seed beam, such that they will bombard its surface with an energy close

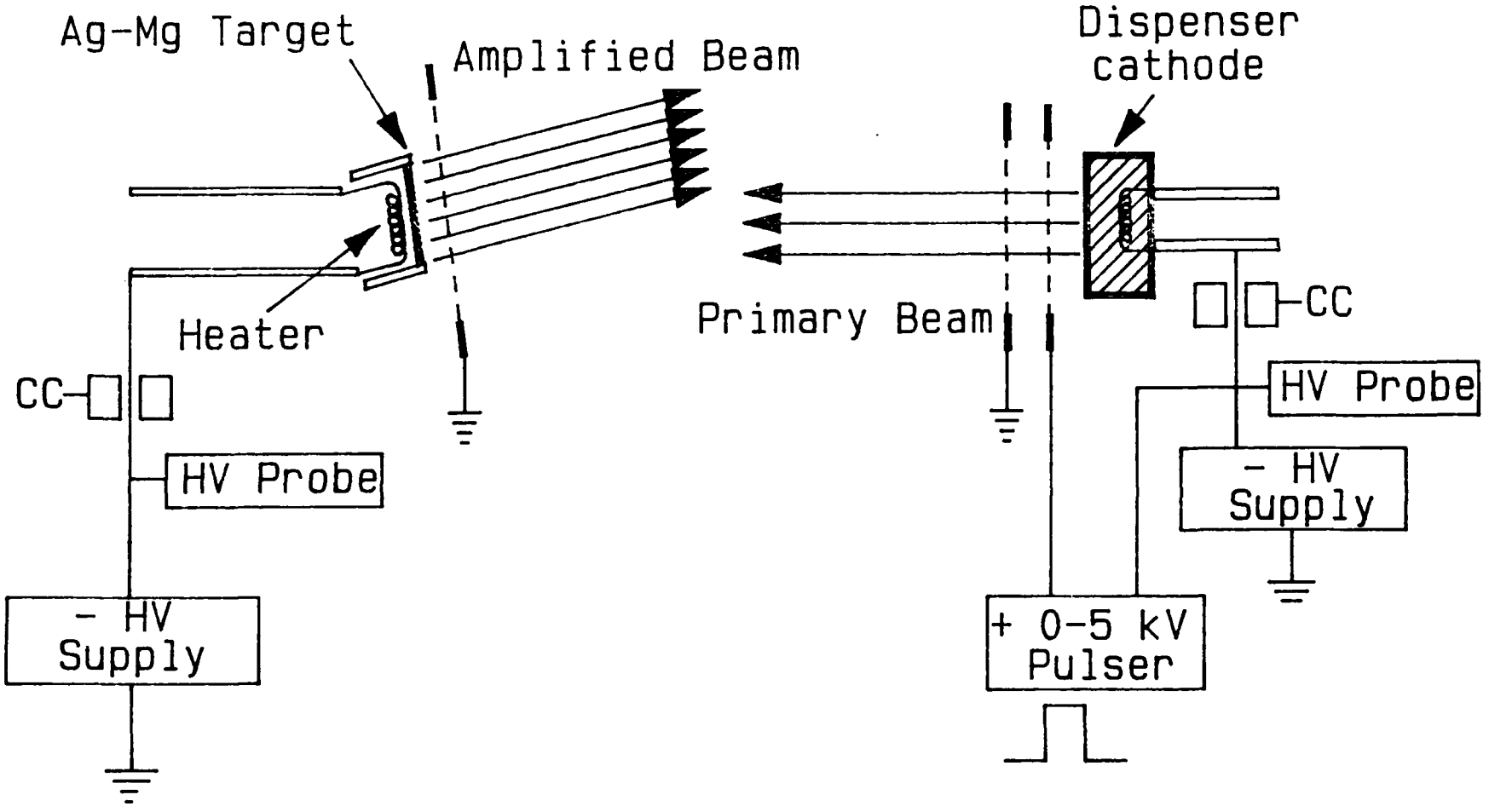

Figure 1. Schematic representation of electron multiplication set up. Current coils are identified by CC. The vacuum chamber is not shown.

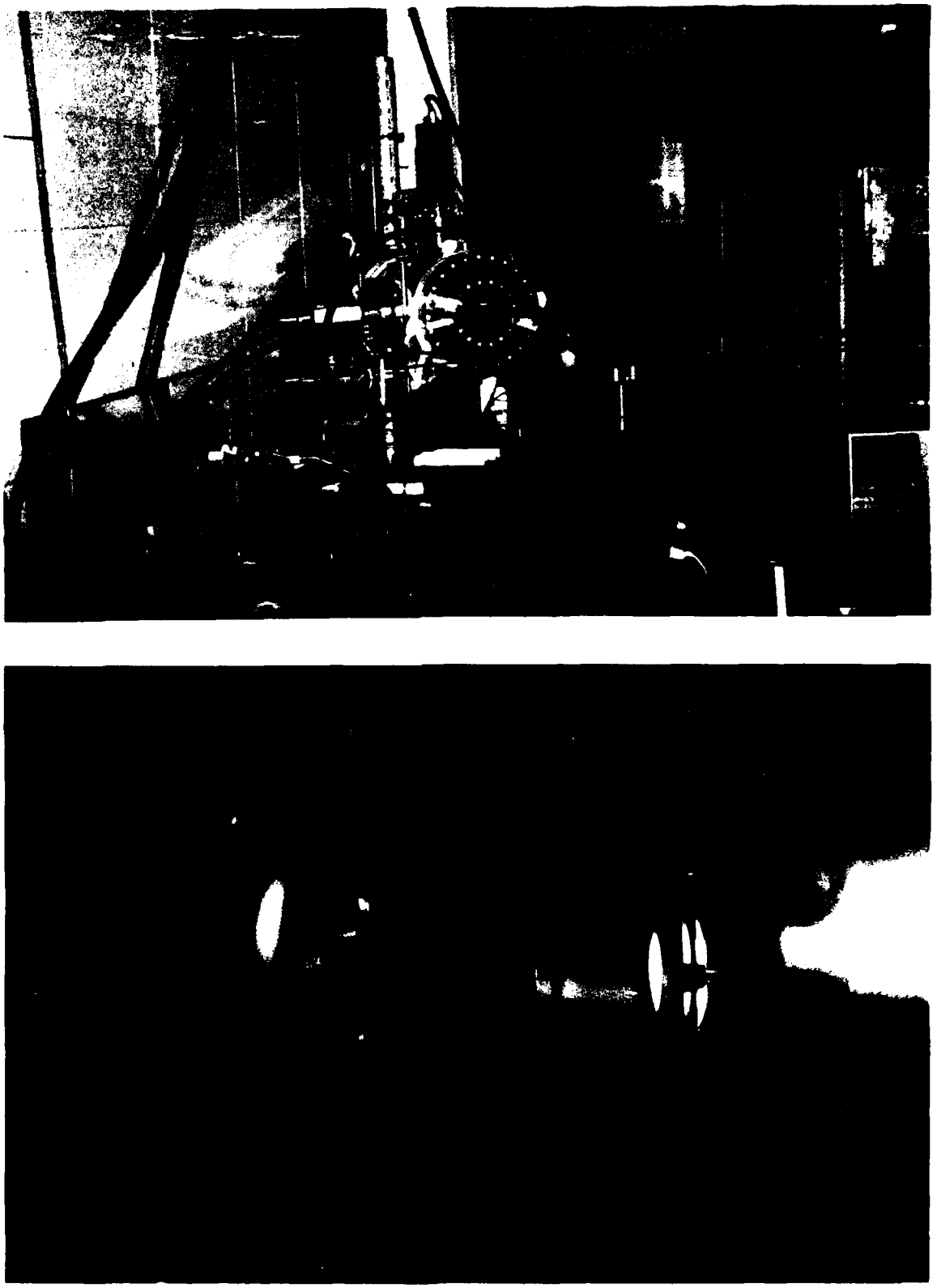

Figure 2. (a) Photograph of the entire system, including the pulser circuit, high voltage, high vacuum feedthroughs, and vacuum chamber. (b) View of the thermionic gun in operation and the target system.

to that necessary for maximum electron yield. The field that decelerates the electrons from the primary beam also accelerates the electrons emitted by the target to form the secondary beam. All grid spacings are such that no space charge limiting occurs on the dispenser or target cathodes.

Electron beam multiplication has been achieved using an activated Ag (98.3%) - Mg (1.7%) polycrystalline alloy target [15]. The target and its corresponding grounded grid are positioned forming an angle with respect to the axis of the primary beam, of either 11^0 or 30^0 to allow extraction of the secondary beam as it will be required in practical applications. An additional benefit of this configuration is that the electron yield is slightly increased with respect to the normal incidence value. The entire setup is enclosed in a stainless steel chamber 20 cm in diameter that is evacuated to a pressure of 1×10^{-7} Torr using a turbomolecular pump. In the electron multiplication experiments, the chamber is filled with 5×10^{-4} Torr of argon to provide quasi-neutralization of the electron streams and thereby overcome the current limitations set by the propagation of unneutralized electron beams in an equipotential region (see section II.2).

To generate the primary electron beam, a circuit was developed that generates a square pulse with pulse-widths ranging from 0.4 to 3 μsec and amplitudes from +0.5 to 5 kV. As illustrated in Figure 1, the pulser is connected between the inner grid and dispenser cathode and both are floated up to -20 kV. The pulser

output is a +0.5 to 5 kV square pulse which allows the generation of an electron pulse. The beam is then further accelerated in the gap between the inner grid and a grounded grid. A detailed schematic of the pulser circuit is illustrated in Figure 3. The krytron pulser is based on modifications to EG&G application note K5502B-3. The pulse repetition rate is controlled by a +6 V clock pulse that controls the gate of the SCR diode (2N1595). The input of the TR131 pulse transformer is obtained discharging a 0.1-mF capacitor by means of an SCR. After the SCR diode closes, the discharging capacitor generates a 1-kV pulse at the output of the pulse transformer. This pulse is the trigger for V1, a KN-29 krytron that controls the rising edge of the pulse by initiating the discharge of capacitor C1 previously charged to 1-5 kV. A second KN-29 krytron, V2, is connected to the cathode of the first one through an RC circuit and when switched on, rapidly completes the discharge of C1 and controls the pulse-width of the high voltage pulse. Figure 4 illustrates a 60-A square current pulse emitted from the thermionic cathode by applying the output of the pulser circuit between the cathode and the inner grid. The entire pulser was powered by an insulation transformer and was floated up to 15 kV. The circuit operated at 1 Hz for more than 300 hours without need of replacing the krytrons.

II.2. Propagation of the primary electron beam

A problem we faced working in vacuum ($P \approx 10^{-7}$ Torr) and at electron beam acceleration energies of approximately 10 keV was the

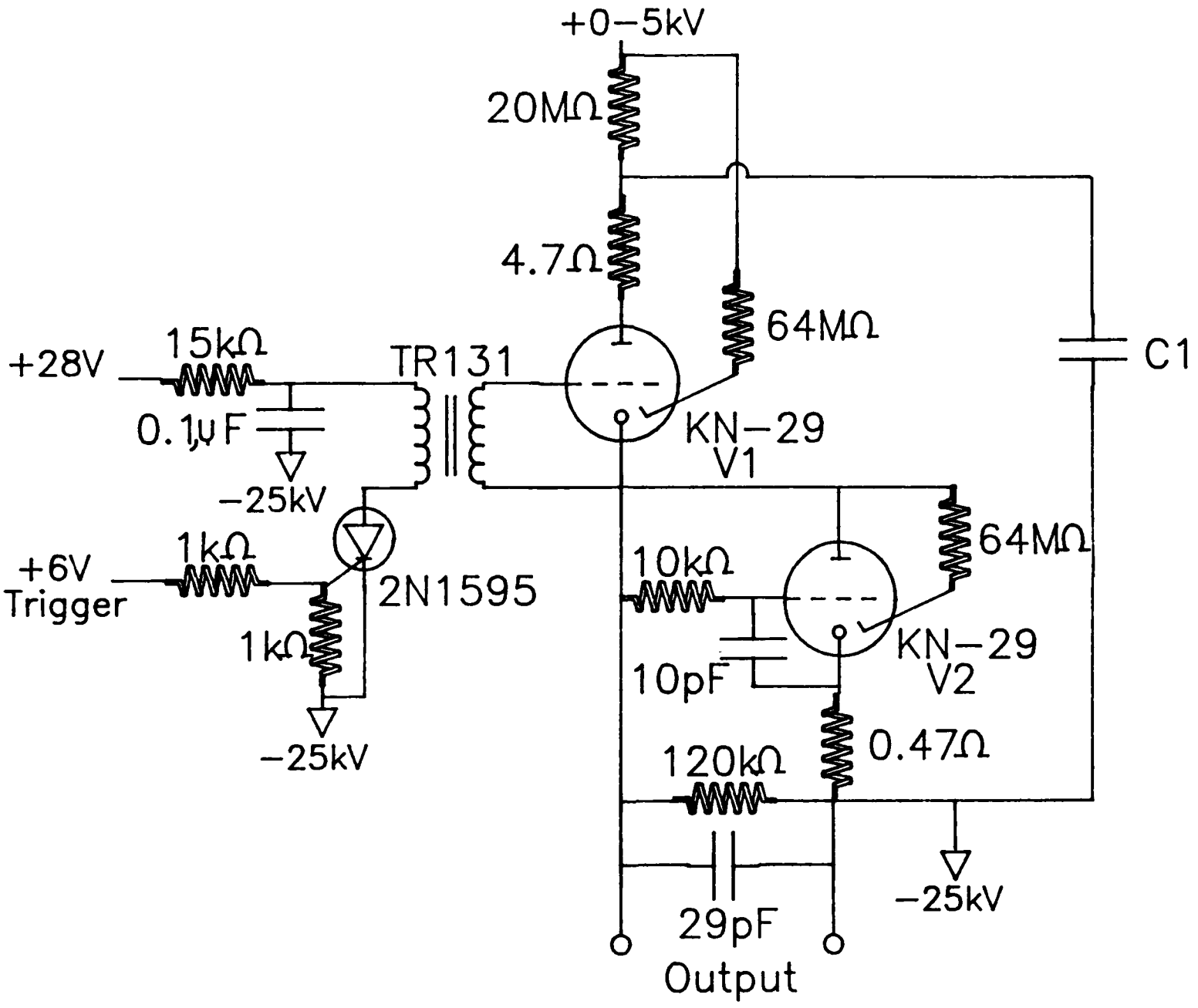

Figure 3. Schematic of the pulser circuit.

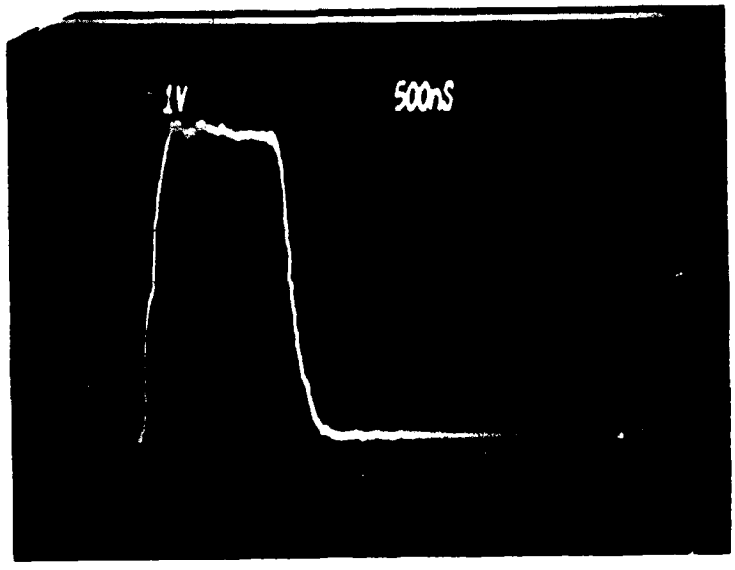

Figure 4. Current pulse emitted from the thermionic cathode. The pulser circuit output voltage is 2.5 kV. 10 A/div, 500 ns/div.

inefficient transmission of the extracted electron gun current to the target through the 15-cm-long drift region defined by the two grounded grids. We observed that the currents reaching the target were almost two orders of magnitude lower than the currents being emitted by the thermionic cathode, under high vacuum conditions (pressures $\approx 10^{-7}$ Torr). We found that the low collected current values due to space charge effects in the drift region, which leads to beam spreading. Adding a small amount of a noble gas in the vacuum chamber (10^{-5} to 10^{-4} Torr of He or Ar) for charge neutralization increased the current reaching the target by more than one order of magnitude. The oscilloscope traces shown in Figure 5 illustrate the drop in the current pulse collected at the target as the argon pressure is reduced from 5×10^{-4} Torr to 5×10^{-6} Torr (the background pressure was 10^{-7} Torr), while Figure 6 is the corresponding collected current vs pressure plot. Argon gas was preferred over helium due to its higher ionization cross section and lower heat conductivity. Helium excessively cooled the thermionic cathode.

II.3. Target Activation

Nonactivated Ag-Mg targets were measured to have electron yields ≤2. The first target surface activation procedure attempted to increase the electron yield consisted in using the Ag-Mg sample as a cathode of a glow discharge in pure oxygen or CO_2 atmospheres to form a high yield oxide layer on the surface. However, for the

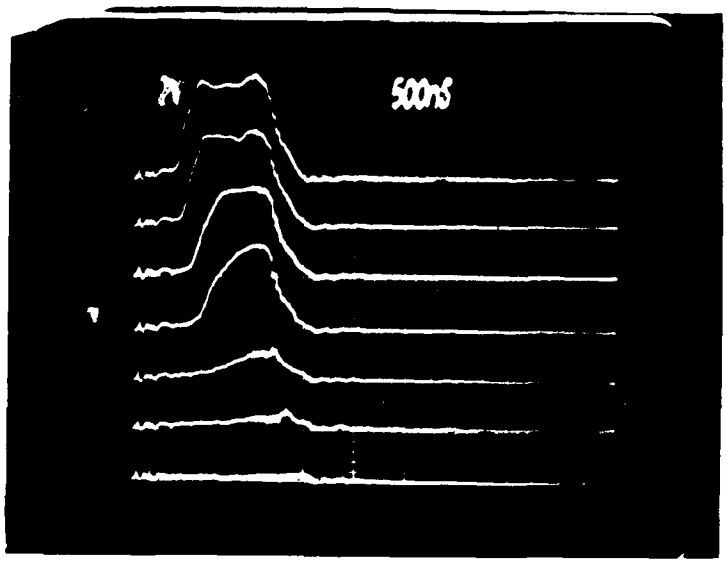

Figure 5. Oscilloscope traces showing the drop of the current pulse collected at the target as the argon pressure is reduced. Primary gun acceleration voltage: 10 kV. The target is grounded. 2 A/div, 500 ns/div. Pressure values corresponding to the traces shown from top to bottom are: 5, 4, 3, 2, 1, 0.5, and 0.05×10^{-4} Torr, respectively.

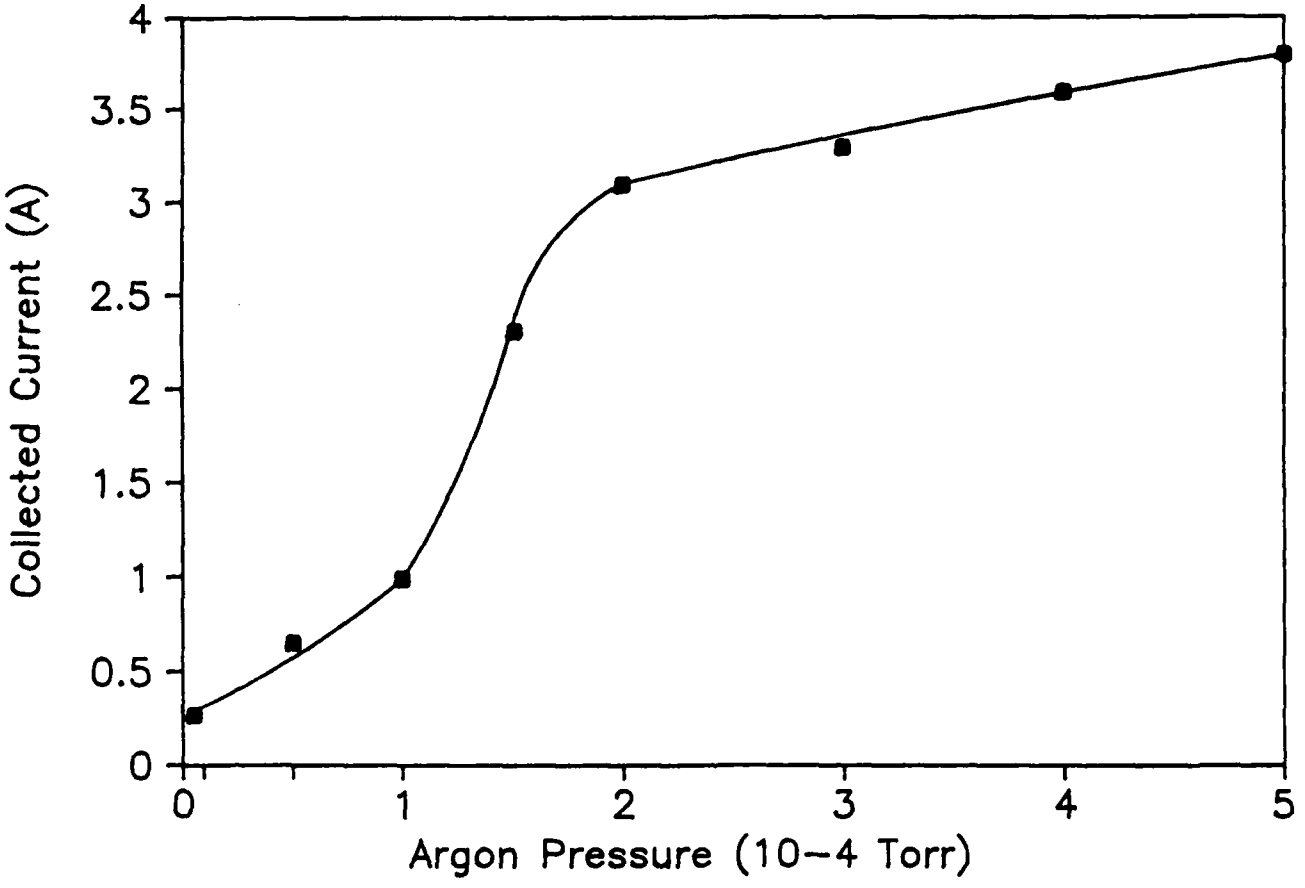

Figure 6. Current pulse collected at the target as a function of argon pressure. The thermionic gun floating voltage is 10 kV. The target is grounded.

range of glow discharge conditions studied (discharge currents from 5 to 20 mA, pressures from 0.8 to 1.1 Torr, and time intervals from 5 to 30 minutes), we were unable to attain electron multiplication factors greater than 2, probably due to a nonoptimized oxide layer thickness or target surface contamination. On the other hand, we obtained electron yields of the order of 5 from a not treated Ag-Mg surface, which could not be reproduced later, probably resulting from a particular not intentionally programmed sequence of events (e.g. pumping, heating with primary gun, BaO evaporation from the dispenser cathode, etc.).

The second activation procedure we attempted consisted of externally heating the sample to favor the migration of Mg to the surface, and then add CO_2 in the vacuum chamber to form a magnesium oxide layer, following a procedure developed to activate dinodes of photomultiplier tubes made of the same material [16]. The initial heating system consisted of a stainless steel (SS) tube which supported the target material, and contained the heater filament external to the high vacuum system as schematically illustrated in Figure 7. The heater filament was placed in soft vacuum (1 mTorr) to reduce oxidation and heat convection losses. However, attempts to reach the desired temperature of 750^{0}C were stalled because of excessive heating of the SS tube, causing a low heating efficiency and contamination of the target surface by the vaporization of SS components.

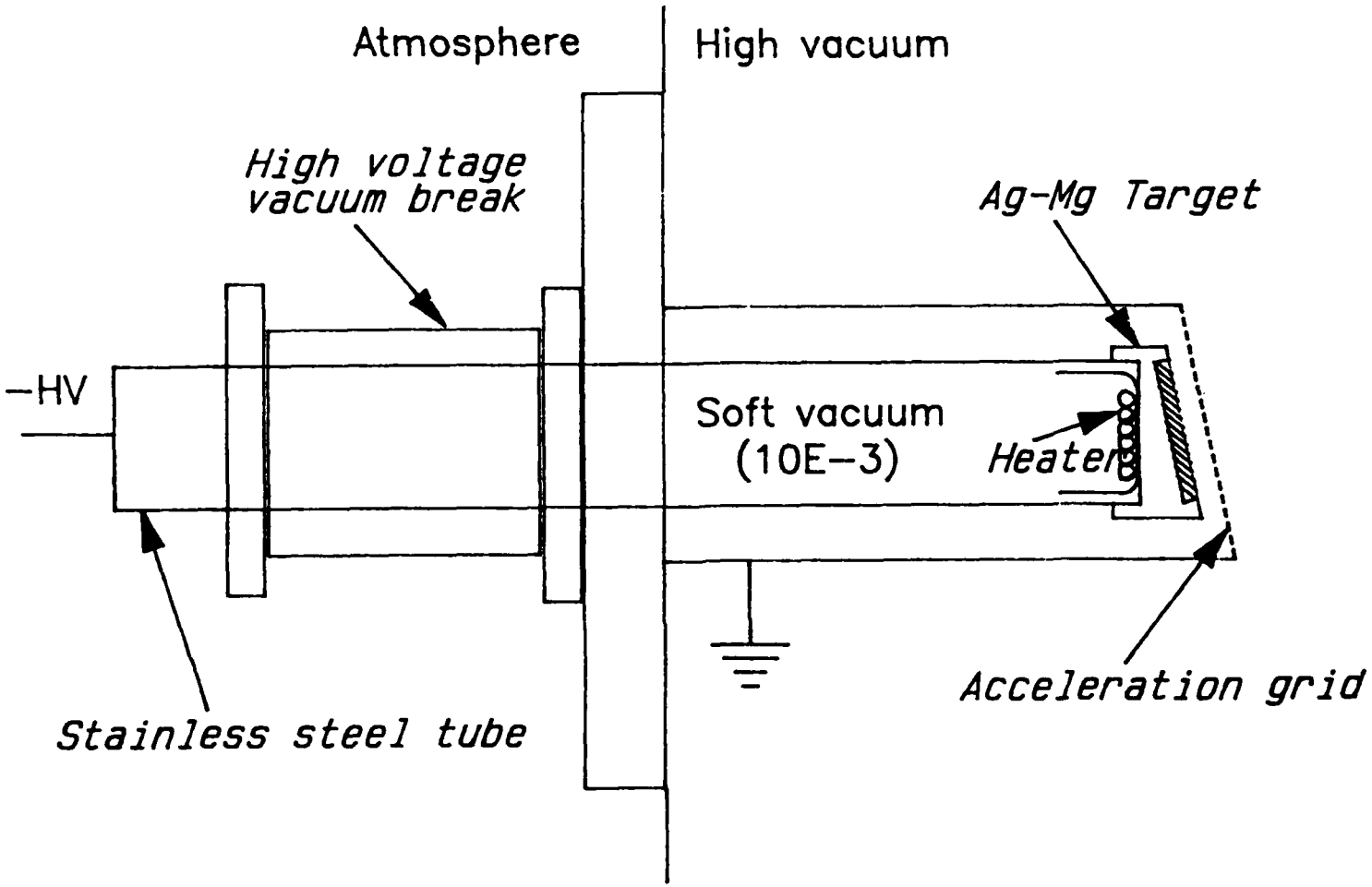

Figure 7. Early design of the heating system used to attempt the Ag-Mg surface activation.

To overcome this problem, we designed a more efficient system of direct heating in which the sample is mounted over the heater (now placed inside the high vacuum chamber) using a supporting molybdenum piece, as shown in Figure 8. The heater filament is potted inside a molybdenum cup and its legs are connected to two high voltage vacuum feedthroughs. The surface temperature of the target was measured using an optical pyrometer through a window installed in one of the ports of the vacuum chamber. The successful activation procedure implemented using this setup is as follows: by increasing the applied ac voltage, a current of 13.5 A is kept constantly circulating through the heater filament until a power of approximately 125 W is dissipated; this process allows to reach 750^{0}C at the target surface after approximately 20 minutes. Then, while keeping the target at this temperature, 400 mTorr of CO_2 are added to the vacuum chamber for 2 minutes, interval after which the gas flow and heating power are interrupted. Failure to activate the target surface was observed to yield multiplication factors of less than 2. After the target temperature was increased to 750^{0}C and exposed for 2 minutes to an atmosphere of 400 mTorr of CO_2, yields of 5 were consistently observed and yields up to 7 have been occasionally measured. Larger yields might result from the optimization of the thickness of the oxide layer, since electron yields up to 12 for lower electron beam current densities have been reported following this procedure [16].

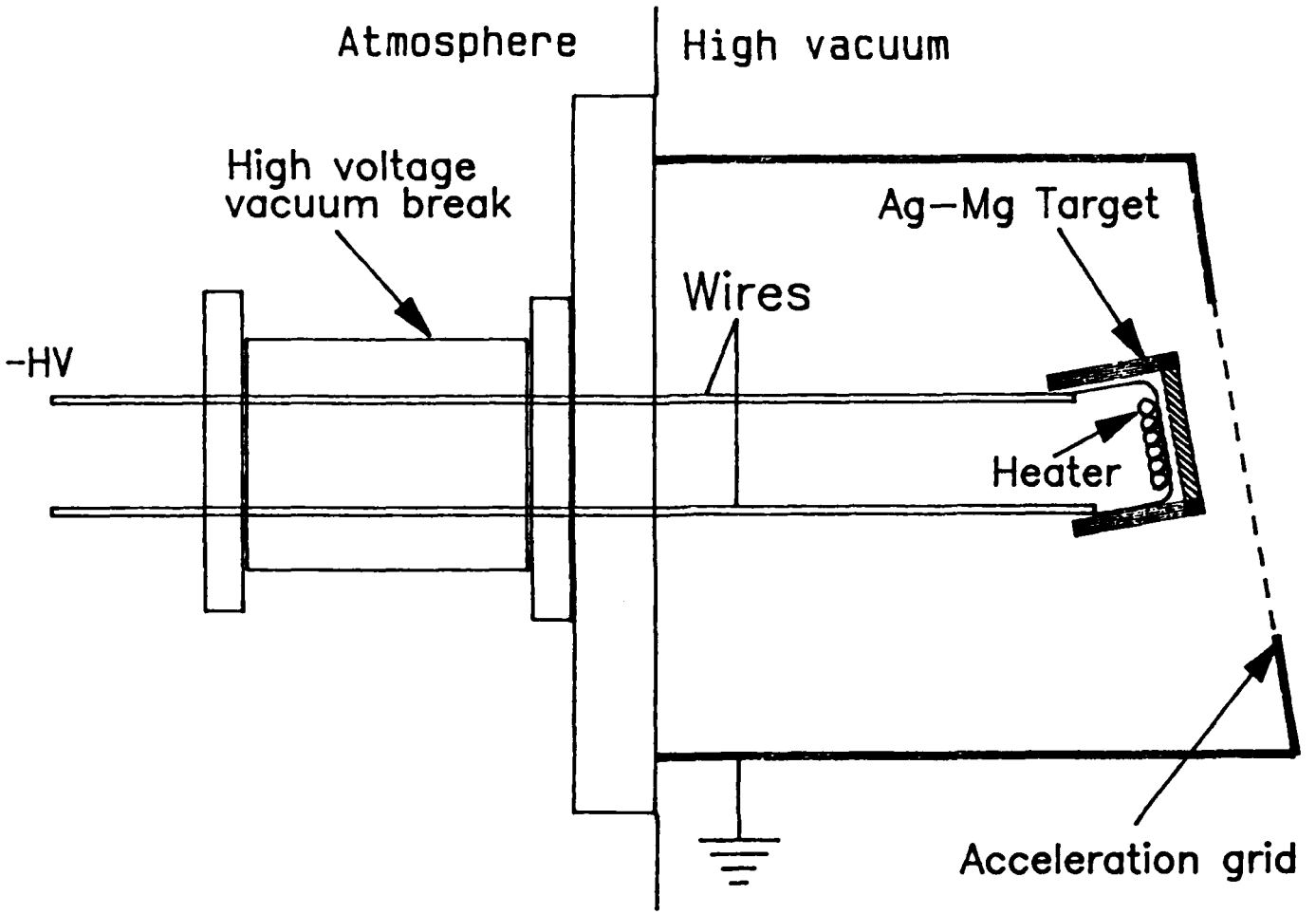

Figure 8. Later design of the heating system succesfully used to activate the Ag-Mg target surface.

III. EXPERIMENTAL RESULTS

III.1. Electron Beam Multiplication

All the electron multiplication experiments were conducted for only one type of target, the Ag-Mg alloy previously described. In Figure 9, are oscilloscope traces showing the effect of electron multiplication. The top trace corresponds to the current pulse collected at the grounded target when bombarded by an 8-keV primary beam impinging at an angle of 30^0. In this situation, the secondary electrons rapidly form a space charge that inhibits significant electron emission, and consequently the target current can be considered a good approximation of the primary beam current impinging on the target if backscattering is neglected [17]. This assumption was verified by applying a 50-V positive bias to the target, in which case the current changed by less than 15 percent. The bottom trace is the measured target current when all conditions are maintained equal, but the target is biased to -5 kV. In this situation, the primary electrons arrive at the target surface with an energy of 3 keV, and the secondary electrons are accelerated to form a 5 keV beam. The bottom trace is the sum of the primary beam current arriving to the target and that of the emitted secondary electron current. Figure 9 shows that for a primary beam current of 2 A. a secondary beam current of 11 A was emitted, corresponding to a multiplication factor of 5.5. The shape of the multiplied electron pulse is observed to follow that of the 1-μsec primary

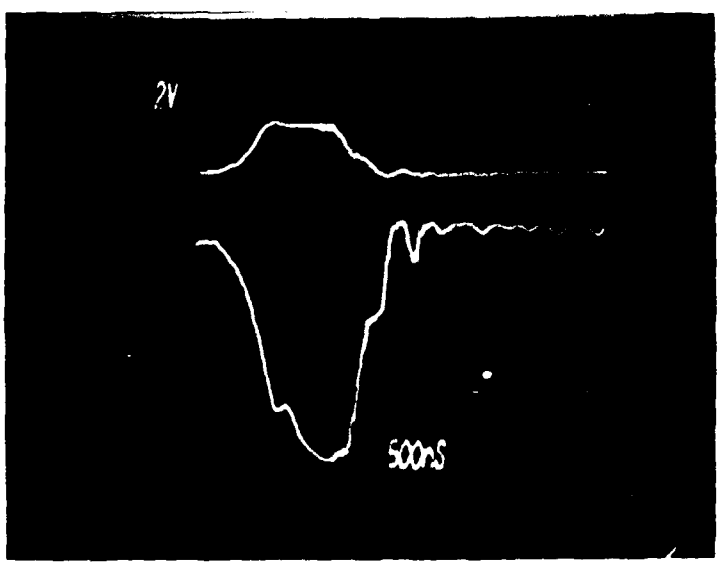

Figure 9. Current flowing to the Ag-Mg target bombarded with an 8-keV electron beam when the target is grounded (upper trace, 2 A/div), and when is biased to -5 kV (lower trace, 2 A/div). The lower pulse represents the sum of the primary beam current collected (positive current) and the emitted current (negative current). The argon background pressure is 5×10^{-4} Torr. The angle between the normal to the target and the axis of the primary beam is 30^0, and the distance between grounded grids is 8 cm.

beam. Impinging on the target with a current of 2.5 A (0.5 A/cm^2) produced 17 A (3.4 A/cm^2) of emitted current when the primary beam had an energy of 8 keV and the target was floated to - 4 kV.

Figures 10(a) and 10(b) show the electron multiplication factors measured as a function of the energy of the primary electrons, for primary beam current densities of 0.3 A/cm^2 and 0.6 A/cm^2 respectively impinging at an angle of 11^0. In both cases, the electron yield is observed to increase from approximately 1 for a 9-keV primary electron energy to nearly 5 for a primary electron energy of about 3 keV. No degradation of the yields was observed to occur after hours of bombardment with μs wide electron beam pulses at a frequency of 1 Hz. Increasing the magnitude of the negative voltage bias of the target such that the primary electrons would arrive at the target surface with an energy of less than the smallest value shown in Figure 10 would probably result in further increase in the yield; however, this was observed to distort the current pulse due to the onset of oscillations.

Figure 11 illustrates the onset of the oscillation for the same primary beam conditions of Figure 9, occurring when the magnitude of the bias is increased by 200 V to -5.2 kV. The emitted target current increases to 13 A, corresponding to an electron multiplication factor of 6.5, before the current pulse is disrupted by oscillations.

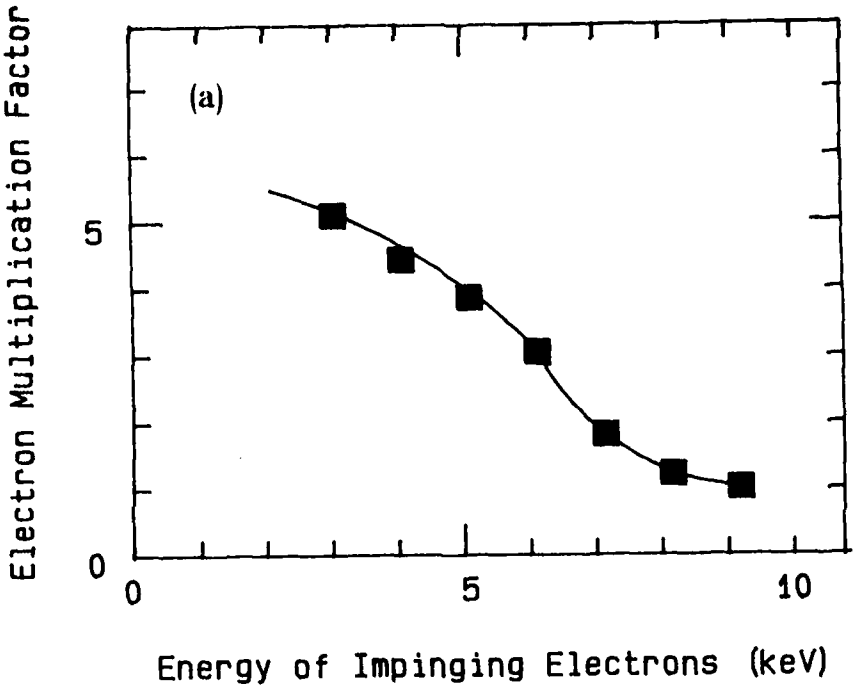

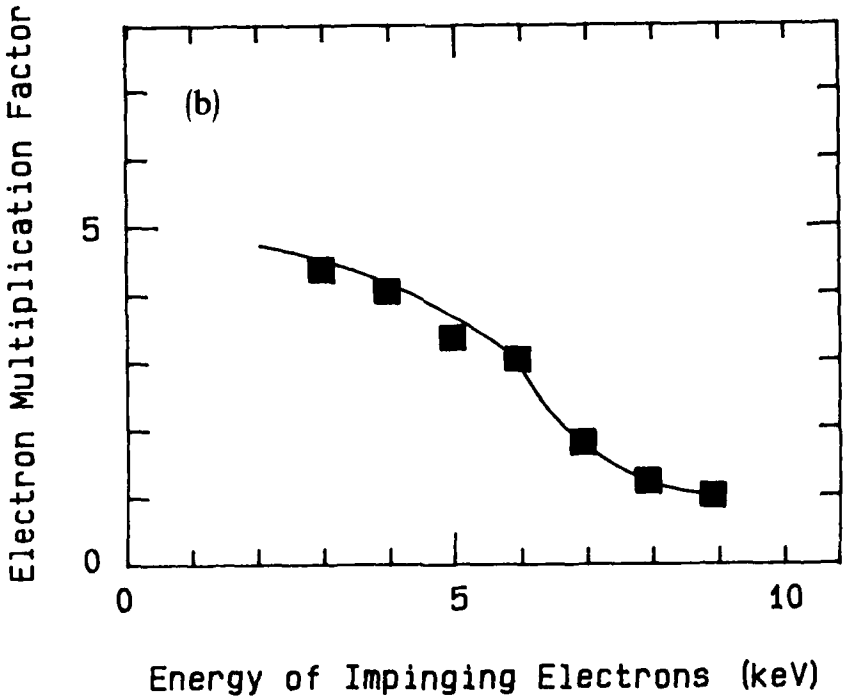

Figure 10. Electron multiplication factors as a function of impinging electron energy for an input current of (a) 1.5 A, and (b) 3.0 A. The angle between the normal to the target surface and the primary beam is 11^0, and the distance between gounded grids is 14 cm.

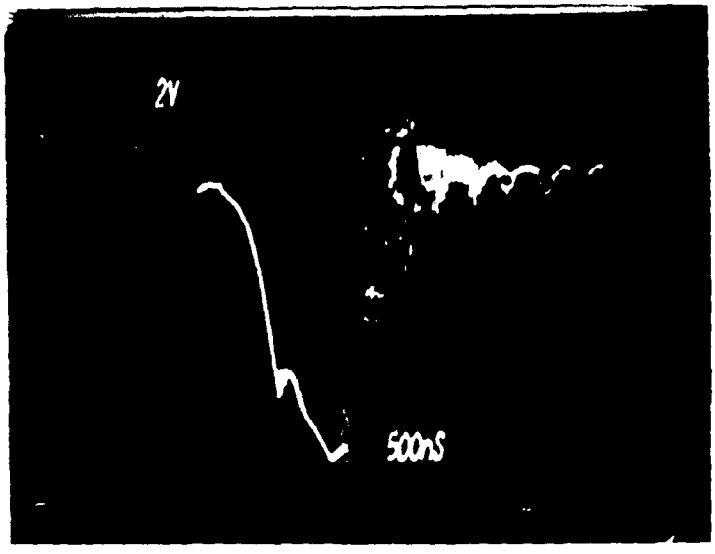

Figure 11. Target current measured for the same primary beam conditions os Figure 9, but biasing the target to -5.2 kV. Oscillations are observed to occur at the end of the emitted current pulse.

III.2. Current oscillations limiting the current density

A detailed experimental study of the frequency, voltage threshold, and dependence on current level and pressure of the observed oscillations was carried on during the final weeks of the project. Figure 12 illustrates the sequence of changes in the target current as the target voltage is varied from 0 to -8 kV, for a primary beam acceleration energy of 10 keV. The target current first changes sign, and then the emitted current continues to increase in magnitude as the impinging energy of the primary electrons approaches the optimum value for electron multiplication (about 1-1.5 keV). However, for V_{target} = -7.5 kV the onset of oscillations on the current pulse can be clearly appreciated, increasing significantly in magnitude for V_{target} = -8 kV. We observed that these oscillations were characterized by a frequency of approximately 25 MHz, almost independent of the current level, acceleration energy or pressure; a typical waveform showing the presence of these oscillations is shown in Figure 13. However, the voltage difference between the target and the floating potential of the thermionic gun corresponding to the onset of the oscillations was observed to be dependent on the conditions; at the working argon pressures of 5×10^{-4} Torr and the target normal at 11^0 respect to the primary beam axis, the oscillations started for an acceleration voltage difference between the primary and secondary beams of approximately 2.5 kV. While at the background chamber pressures of 10^{-7} Torr, they started for a voltage difference lower than 1 kV. It is important, however, to consider that the latter

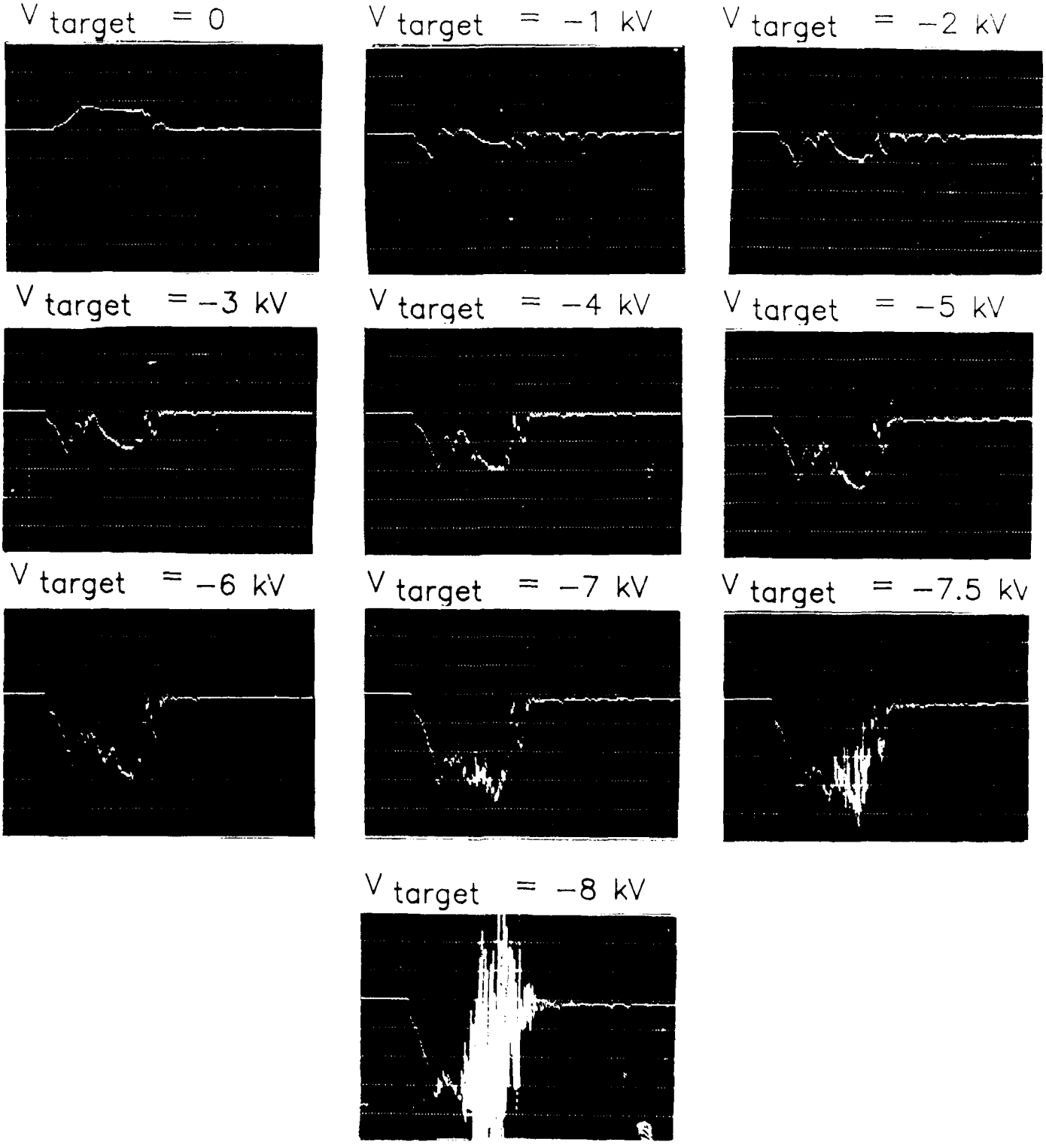

Figure 1. Sequence illustrating the changes in target current as the target voltage is varied from 0 to −8 kV. [illegible] kV. Argon pressure is [illegible] torr. [illegible]

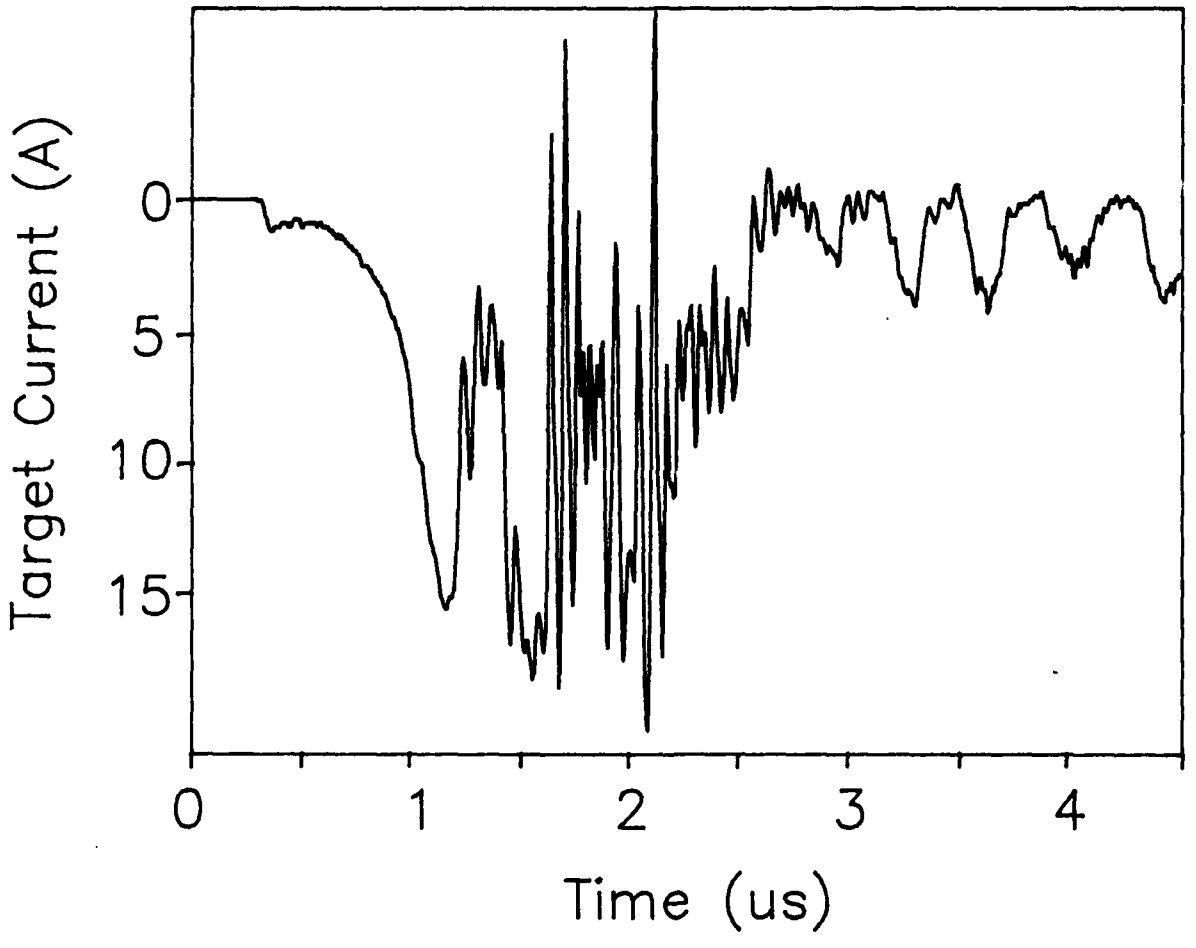

Figure 13. Time evolution of the target current pulse showing the presence of oscillations. The signal was digitalized in 1,024 channels with 5-ns resolution. The primary beam current is 2 A. V_{acc} = 7 kV. The target floating potential is 4 kV. Argon pressure is 5×10^{-4} Torr.

condition corresponds to current values one order of magnitude lower because of the poor neutralization of the electron beams.

To study the propagation of the primary and secondary electron beams in the drift region, we constructed and mounted a vacuum ready, movable, self-integrating Rogowski coil (3 cm in diameter) in front of the target system. The design of the coil is shown in Figure 14. Figure 15 shows the current pulse collected at the grounded target (top trace) and the current measured with the Rogowski coil. In this way, we were able to monitor the primary beam arriving to the target system and the sum of the counter-propagating primary and secondary electron beam currents. The coil showed the same type of current oscillations measured in the propagating beam as in the target current. These measurements, however, were not conclusive in clarifying the nature of the current oscillations due to the difficulty to attain an adequate target activation, probably originated by the outgassing of the coil's aluminum shielding when the target was heated to 750^{0}C as required for activation. This contamination was observed even when the coil was retracted 10 cm during target activation.

The possibility of the current oscillations being originated in the target gap was studied. The space charge accumulation in the target gap was calculated numerically to identify a possible field inversion in that gap when the primary beam is decelerated to the optimum impinging energy. The oblique incidence of the primary electrons and the presence of emitted secondaries were taken into

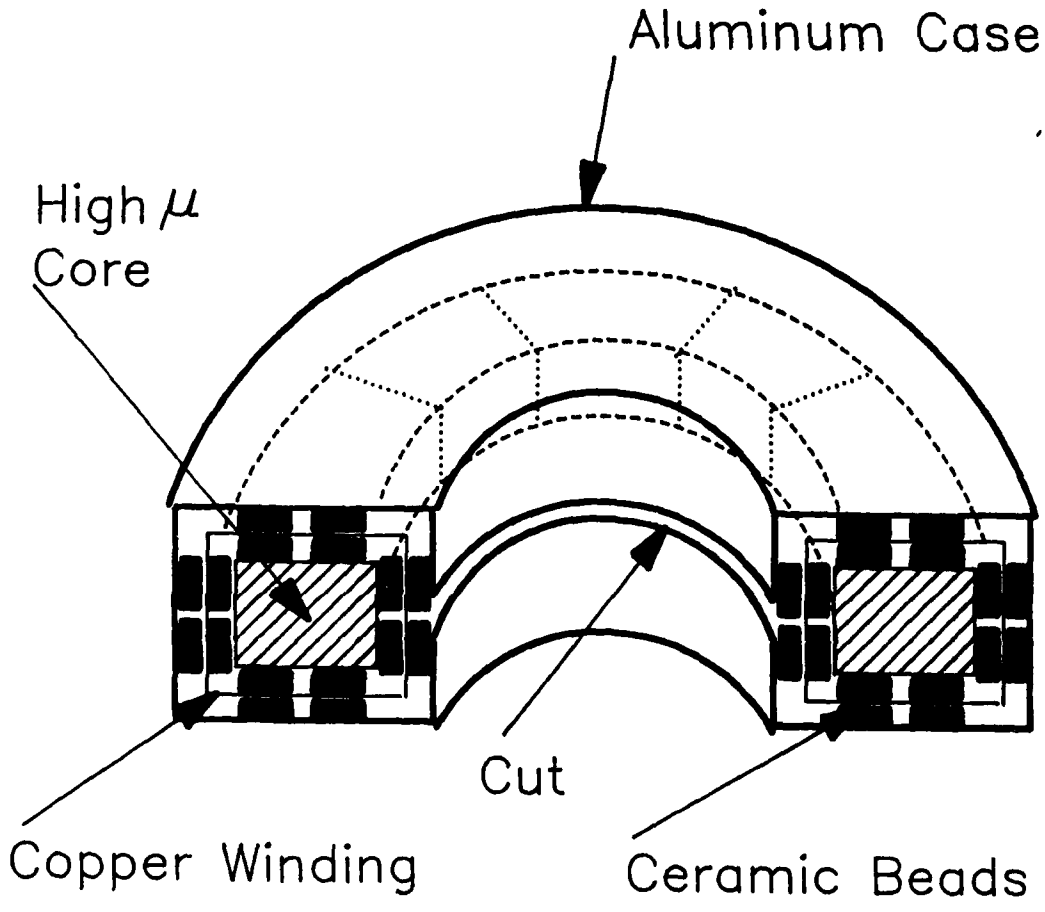

Figure 14. Schematic view of the high vacuum, self-integrating Rogowski coil constructed to study the propagation of the electron streams in the drift region.

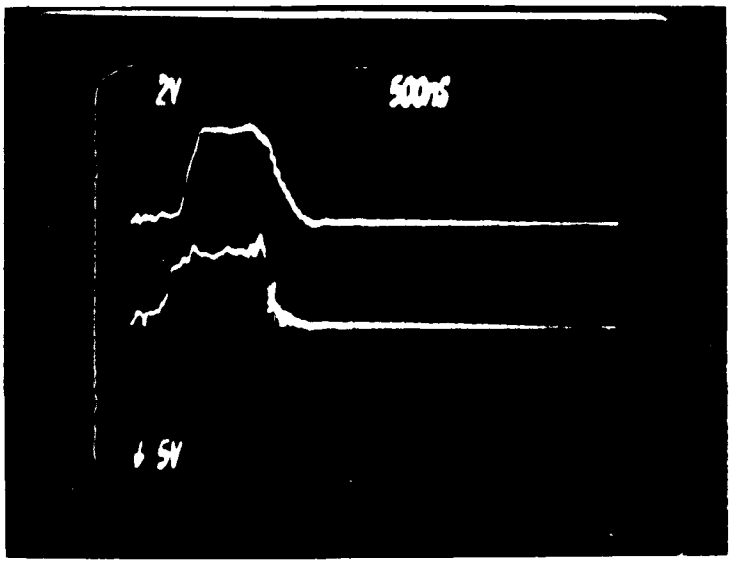

Figure 15. Current pulse collected at the grounded target (top trace, 2 A div) and corresponding current measured by the Rogowski coil (bottom trace, 4 A/div) placed in front of the target system. V_{acc} = 10 kV. Argon pressure is 5×10^{-4}.

account. These calculations showed that no such field inversion can be expected as long as the emitted current density is below the Child-Langmuir current limit for that gap, a condition that was satisfied in our experimental situation. Also, the relative independence of the onset of oscillations on the current density level indicates that space charge effects in the target gap are not likely to be responsible for these oscillations.

If the observed oscillations are not generated by space charge effects in the target acceleration gap, they should originate in the drift region where the electron beams propagate. Instabilities in a neutralized electron stream propagating in a drift tube have been widely observed by different authors and predicted and modeled theoretically [18-23]. For instance, the well known Pierce instability [22], characterized by a critical perveance of approximately 190×10^{-6} $A/V^{3/2}$ for its onset, might be inferred as a double streaming growth (due to interaction between the electron stream and the ions), or due to the interaction between the electron stream and charges on the grids and drift tube walls [23]. However, this critical perveance value is well above our maximum perveance values ($I \approx 10$ A, $V = 10^4$ V) of 10×10^{-6} $A/V^{3/2}$, and also its onset should be strongly dependent on the acceleration voltage, which was not observed in our experiments.

Besides, the observed frequency of oscillations does not seem to be easily related to any natural oscillation frequency of the electron beam produced plasma in the drift region. The electronic

plasma frequency $f_{pe} = 1/2\pi\ (n_e\ e^2\ /m_e\ \Sigma_0)^{1/2}$ can be estimated calculating n_e as $n_e = j_{beam} / e\ v_e$ where j_{beam} is the electron beam current density, and $v_e = (2\ e\ V_{ac} / m_e)^{1/2}$ is the electron beam velocity. For typical values of $j_{beam} = 1\ A/cm^2$, $V_{ac} = 10^4\ V$, results $n_e \approx 10^9\ cm^{-3}$, and $f_{pe} \approx 290$ MHz, which is much higher than the observed frequency $f_{osc} \approx 25$ MHz. On the other hand, the ion plasma frequency $f_{pi} = (m_e/m_i)^{1/2}\ f_{pe} \approx 3.7 \times 10^{-3}\ f_{pe} = 1.1$ MHz $<<$ f_{osc}. The absence of any applied magnetic field precludes the presence of low frequency oscillations originated in the beating of high frequency axial modes [24].

In consequence, by the end of the project, the origin and eventual remedy of the observed oscillations remains unclear. Nevertheless, a substantial increase in the acceleration voltage might solve this limitation on the maximum current densities attainable using this scheme. A more detailed study of the onset of oscillations for higher ($>$ 15 kV) acceleration voltages could not be completed due to the occurrence of arcs to the grounded grids in the thermionic and target systems, only solvable through a major design change, that was not possible to complete during the period of the contract.

IV. CONCLUSIONS

The experiments performed during this contract demonstrate that multiplication of electron beams in high yield targets is a viable method for the generation of high current density electron beams. The experiments were limited to bombardment of an activated

Ag-Mg alloy. After activation, this type of target was measured to consistently have electron yields greater than 5, with yields up to 7 being occasionally observed. No degradation of the electron yields were observed to occur after hours of bombardment with a 0.5-A/cm^2, 1-μs-wide electron beam pulses at a frequency of 1 Hz. A systematic optimization of the activation procedure was not completed to optimize the thickness of the oxide layer, and higher yields may be possible. Other materials not explored during this contract, such as cesium coated semiconductors, have been measured to provide yields larger than 100 for the small electron current densities typical of photomultiplier tubes and might have potential to yield significantly higher electron beam multiplication factors.

Using Ag-Mg targets 2.5 cm in diameter, we were able to generate a 17- electron beam pulse, 1 μs wide by multiplication of a 2.5-A beam. The maximum current obtained was limited by the onset of oscillations in the electron beam current. The oscillations are probably due to electron-ion instabilities known to occur in the propagation of quasi-neutralized electron streams. In this case, the onset of instabilities could be shifted to much higher current values by increasing the electron beam acceleration potential, which in the current experiment was limited to 10 kV. Once this limitation is overcome, based on the results discussed herein it should be viable to obtain very large current density electron beams by multiplication of highly controllable, low current density beams.

REFERENCES

1) C. Murray, B. Szapiro, J.J. Rocca, Appl. Phys. Lett. 54, 2303, 1989.

2) V.K. Zworykin and E.G. Ramberg, Photoelectricity and Its Applications, J. Wiley and Sons, Inc., New York, 1949.

3) G.W. McClure, Phys. Rev., 124, 969, 1961.

4) R.A. Dugdale, J. Mater. Sci., 10, 896, 1975.

5) J.J. Rocca, J.D. Meyer, M.R. Farrell and G.J. Collins, J. Appl. Phys., 56, 790, 1984.

6) W.M. Clark, Jr. and G.J. Dunning, J. Quantum Electron., QE-14, 126, 1978.

7) B. Wernsman, H.F. Ranea-Sandoval, J.J. Rocca, and H. Mancini, IEEE Transactions on Plasma Science, PS-14, 518, 1986.

8) H.F. Ranea-Sandoval, N. Reesor, B.T. Szapiro, C. Murray, and J.J. Rocca, IEEE Transactions of Plasma Science, PS-15, 361, 1987.

9) H.C. Bourne, Jr., R.W. Cloud, and J.G. Trump, J. Appl. Phys., 26, 596, 1955.

10) B. Szapiro, J.J. Rocca, and T. Prabhuram, Appl. Phys. Lett., 53, 358, 1988.

11) Chunghsin Lee, Appl. Phys. Lett., 44, 565, 1983.

12) C.H. Lee and P.E. Oettinger, IEEE Transactions on Nucl. Sci., NS-32, 3045, 1985.

13) Cathode Standard 1000, Spectra-Mat, Inc., 1240 Highway, Watsonville, CA 95076.

14) Buckbee Mears, 245 E 6th St, St. Paul, MN 55101.

15) Monocrystals Co., 1721 Sherwood Blvd., Cleveland, OH 44117.

16) P. Wargo, B.V. Haxby, and W.G. Shepherd, J. Appl. Phys., 27, 1311, 1956.

17) Electron backscattering for a magnesium oxide surface should be of the order of 10 percent. L.N. Dobretsov and M.V. Gomoyunova, Emission Electronics, page 254, Keter Press, Jerusalem, 1971.

18) J.R. Pierce, Theory and Design of Electron Beams, D. Van Nostrand, New Jersey, 1954.

19) J.R. Pierce. J. Appl. Phys., 19, 231, 1947.

20) V.D. Fedorchenko, B.N. Rutkevich, V.I. Muratov, and B.M. Chernyi, Sov. Phys.-Tech. Phys., 7, 696, 1963.

21) M.V. Nexlin, M.I. Taktakishvili, and A.S. Trubnikov, Sov. Phys. JETP, 33, 548, 1971.

22) J.R. Pierce, J. Appl. Phys. 21, 1063 (1950).

23) J. Frey and C.K. Birdsall, J. Appl. Phys. 37, 2051 (1966).

24) S.A. Self, ' ppl. Phys. 40, 5232 (1969).

Electron beam generation by electron multiplication

C. Murray, B. Szapiro,[a] and J. J. Rocca[b]
Electrical Engineering Department, Colorado State University, Fort Collins, Colorado 80523

(Received 13 February 1989; accepted for publication 27 March 1989)

We have demonstrated that intense pulsed electron beams can be created by multiplication of lower current electron streams impinging on a high electron yield target. A 17 A electron beam of 1 μs pulse width was generated from a 2.5 A beam bombarding an activated Ag-Mg target 2.5 cm in diameter.

We have demonstrated a new approach for the generation of broad-area intense electron beams based on the multiplication of electron streams achieved by bombarding high-yield materials. This well known phenomenon has been employed for decades in photomultiplier detectors to amplify currents in the submilliamp range,[1] but to our knowledge has never been used for the generation of intense electron beams. We report the generation of broad-area electron beam pulses of 1 μs duration with current densities up to 3.4 A/cm^2 by single-stage multiplication of a 0.5 A/cm^2 electron stream. The scheme has the potential of generating intense electron beams whose current and pulse width are tailored by controlling a low current density beam.

Ion and photon fluxes have been previously used to cause intense electron emission from cold cathodes. The emission of electrons from cathode materials following the bombardment by energetic ions has been widely used in the generation of broad-area electron beams.[2-7] While many cathode materials exist which present high electron yields following the bombardment by ions,[8,9] ion bombardment electron guns have limitations for the generation of very high current density beams. For a given electron yield, the electron beam current density is limited by the bombarding ion flux, which is itself limited by the large positive space charge. Also, ion bombardment induced sputtering of the cathode material is an undesirable effect that is present and limits the electron gun lifetime. Recently, very large electron beam current densities have been achieved using photocathodes.[10,11] The photoemission scheme has the advantages that photons do not present space-charge limitations or cause sputtering. An additional advantage of photocathodes is the very small energy spread of the emitted beam produced by monochromatic irradiation. However, the laser required as a photon source increases the size and complexity of the cathode, and also limits its scaling to very broad areas.

In the experiments reported herein, an electron beam was generated by electron bombardment induced emission of an activated Ag-Mg target 2.5 cm in diameter. In this scheme the electrons emitted by a low current density primary electron source impinge on a high electron yield target at an energy close to that required for maximum emission of secondary electrons. The secondary electrons are subsequently accelerated in the opposite direction to form a higher current density beam. Electrons cause negligible sputtering and create a space charge which is two orders of magnitude lower than that corresponding to an ion beam of the same flux and energy. The experiments reported in this letter show that some of the same materials and surface activation procedures developed for electron multiplication of the microamp level in photomultiplier tubes allow for efficient electron multiplication at current densities many orders of magnitude larger. Consequently, the scheme reported herein has the potential of generating very high current density electron beams.

The setup used to demonstrate this electron beam generation scheme is represented in Fig. 1. The primary, or seed, electron beam pulse is generated from a 2.5-cm-diam thermionic dispenser cathode, by pulsing an accelerating grid to positive potential with respect to the cathode and floating them negatively with respect to a grounded grid. The beam propagates to another grounded grid placed in close proximity with the target. The target is negatively biased with respect to ground to retard the electrons from the seed beam, such that they will bombard its surface with an energy close to that necessary for maximum electron yield (about 1 keV for Ag-Mg targets). Electron beam multiplication has been achieved using an activated Ag (98.3%)-Mg (1.7%) polycrystalline alloy target. The target and its corresponding grounded grid are positioned forming an angle with respect to the axis of the primary beam, either 11° or 30° in the experiments reported herein, to allow extraction of the secondary beam as it will be required in practical applications. An additional benefit of this configuration is that the electron yield is slightly increased with respect to the normal incidence value. The entire setup is enclosed in a stainless-steel chamber 20 cm in diameter that is evacuated to a pressure of 1×10^{-7} Torr using a turbomolecular pump. In the electron

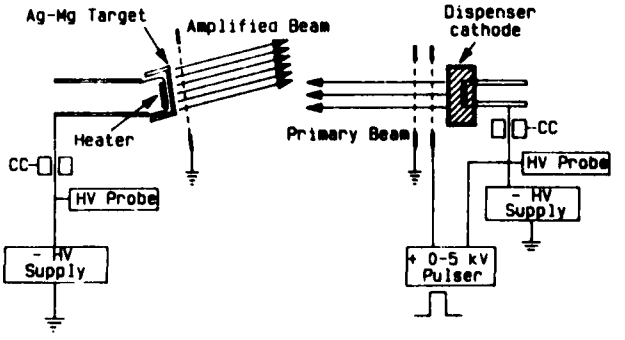

FIG. 1. Schematic representation of electron multiplication setup. Current coils are identified by CC. The vacuum chamber is not shown.

[a] Postdoctoral Fellow, University of Buenos Aires.
[b] National Science Foundation Presidential Young Investigator.

 0003-6951/89/232303-03$01.00

multiplication experiments the chamber is filled with 5×10^{-4} Torr of argon to provide quasineutralization of the electron streams and thereby overcome the current limitations set by the propagation of unneutralized electron beams of less than 10 keV in an equipotential region.[12]

The Ag-Mg target surface was activated to obtain large electron yields following a procedure developed to activate dynodes of photomultiplier tubes made of the same material.[13] The procedure consists in diffusing Mg to the surface by heating the target and achieving oxidation in a CO_2 atmosphere to form a magnesium oxide layer. Failure to activate the target surface was observed to yield multiplication factors of less than 2. After the target temperature was increased to 750 °C and exposed for 2 min to an atmosphere of 400 mTorr of CO_2, yields of five were consistently observed and yields up to seven have been occasionally measured. Higher yields might result from the optimization of the thickness of the oxide layer; a systematic optimization of the activation procedure has not yet been completed.

In Fig. 2 the oscilloscope traces show the effect of electron multiplication. The top trace corresponds to the current pulse collected at the grounded target when bombarded by an 8 keV primary beam impinging at at angle of 30°. In this situation the secondary electrons rapidly form a space charge that inhibits significant electron emission and consequently the target current can be considered a good approximation of the primary beam current impinging on the target if backscattering is neglected.[14] This assumption was verified by applying a 50 V positive bias to the target, in which case the current changed by less than 15%. The bottom trace is the measured target current when all conditions are maintained equal, but the target is biased to -5 kV. In this situation the primary electrons arrive at the target surface with an energy of 3 keV and the secondary electrons are accelerated to form a 5 keV beam. The bottom trace is the sum of the primary beam current arriving to the target and that of the emitted secondary electron current. Figure 2 shows that for a primary beam current of 2 A a secondary beam current of 11 A was emitted, corresponding to a multiplication factor of 5.5. The shape of the multiplied electron pulse is observed to follow that of the 1 μs primary beam. Impinging on the target with a current of 2.5 A (0.5 A/cm^2) produced 17 A (3.4 A/cm^2) of emitted current when the primary beam had an energy of 8 keV and the target was floated to -4 kV.

Figures 3(a) and 3(b) show the electron multiplication factors measured as a function of the energy of the primary electrons, for primary beam current densities of 0.3 and 0.6 A/cm^2, respectively, impinging at angle of 11°. In both cases the electron yield is observed to increase from approximately one for a 9 keV primary electron energy to nearly five for a primary electron energy of about 3 keV. No degradation of the yields was observed to occur after hours of bombardment with μs-long electron beam pulses at a frequency of 1 Hz. Increasing the magnitude of the negative voltage bias of the target such that the primary electrons would arrive at the target surface with an energy of less than the smallest value shown in Fig. 3 would probably result in further increase in the yield; however, this was observed to distort the current pulse due to the onset of oscillations.

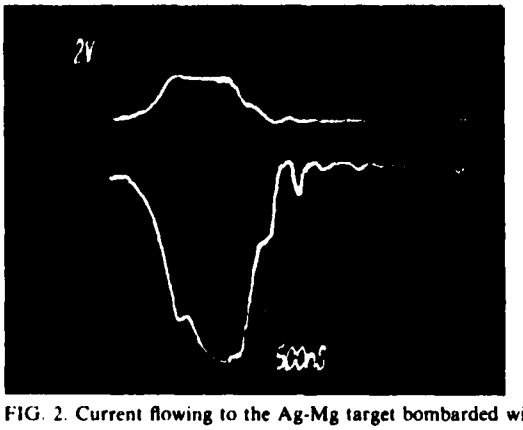

FIG. 2. Current flowing to the Ag-Mg target bombarded with an 8 keV electron beam when the target is grounded (upper trace, 2 A/div) and when it is biased to -5 kV (lower trace, 2 A/div). The lower pulse represents the sum of the primary beam current collected (positive current) and the emitted current (negative current). The background pressure of argon is 5×10^{-4} Torr. The angle between the normal to the target and the axis of the primary beam is 30°, and the distance between grounded grids is 8 cm.

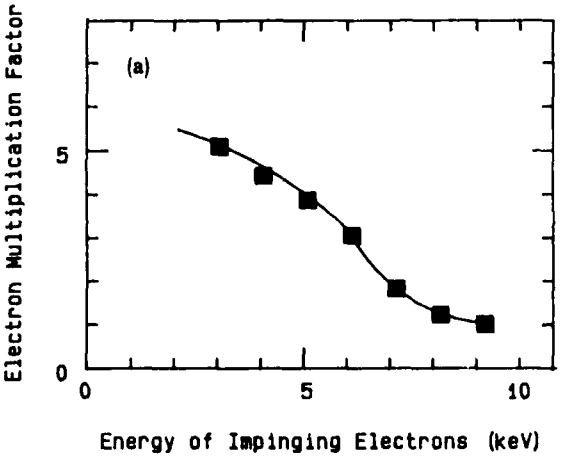

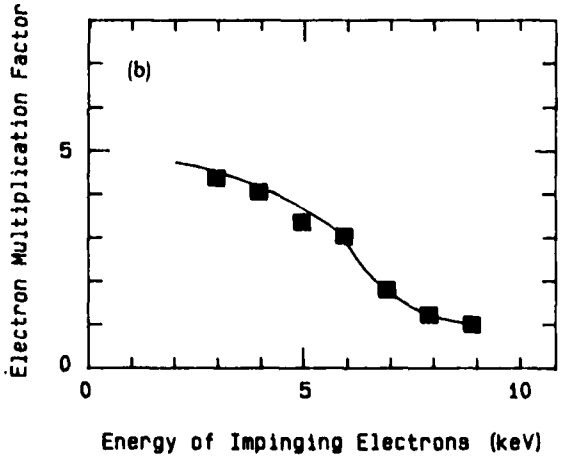

FIG. 3. Electron multiplication factors as a function of impinging electron energy for an input current of (a) 1.5 and (b) 3.0 A. The angle between the normal to the target surface and the primary beam is 11°, and the distance between grounded grids is 14 cm.